

## Ultimate Energy Density of Observable Cold Baryonic Matter

James M. Lattimer and Madappa Prakash

*Department of Physics and Astronomy, Stony Brook University, Stony Brook, New York 11794-3800, USA*  
(Received 10 November 2004; published 24 March 2005)

We demonstrate that the largest measured mass of a neutron star establishes an upper bound to the energy density of observable cold baryonic matter. An equation of state-independent expression satisfied by both normal neutron stars and self-bound quark matter stars is derived for the largest energy density of matter inside stars as a function of their masses. The largest observed mass sets the lowest upper limit to the density. Implications from existing and future neutron star mass measurements are discussed.

DOI: 10.1103/PhysRevLett.94.111101

PACS numbers: 26.60.+c, 21.65.+f, 97.60.Jd

The number of neutron stars with measured masses has grown in recent years [1,2]. The most accurately measured masses are from timing observations of radio binary pulsars [3] and, until recently, were consistent with neutron star masses in the range  $1.26$  to  $1.45M_{\odot}$  [1]. Recent data on binaries containing pulsars and white dwarfs, however, indicate a larger range of masses [2]. An example is the binary containing PSR J0751 – 1807, with  $2.2 \pm 0.2M_{\odot}$  with  $1\sigma$  errors [4]. Data from x-ray binaries [1] also suggest a wide range in masses but are subject to greater theoretical and observational uncertainties. As neutron stars are expected to contain the densest cold baryonic matter outside black holes, the maximum neutron star mass and the corresponding maximum energy density are of great interest.

We demonstrate here that a precisely measured neutron star mass sets an upper limit to the mass density, or, equivalently, the energy density, inside the star. The larger the measured mass, the smaller the density limit. A sufficiently large mass could delimit classes of possible equations of state (EOS). A limit for this maximum density is proffered utilizing an analytic solution of Einstein's equations. This limit is checked by comparing numerical results for a variety of EOS of both normal and self-bound stars. Recent neutron star mass measurements are summarized and inferences drawn.

From the general relativistic structure equations [5,6], the maximum compactness of a star is set by the limit  $R > (9/4)GM/c^2$  [7], where  $R$  and  $M$  are the stellar radius and mass, respectively. With the additional requirements that (i) nowhere in the star is the speed of sound  $c_s$  greater than the speed of light  $c$ , (ii)  $c_s$  is everywhere real, and (iii) the EOS matches smoothly to calculable low density EOS near the nuclear saturation density  $\rho_s \approx 2.6 \times 10^{14} \text{ g cm}^{-3}$ , Ref. [8] showed that the compactness limit is increased to

$$R \geq 2.94GM/c^2. \quad (1)$$

This result improves the limit  $R \geq 3.05GM/c^2$  established [9] using the prescription  $c_s = c$  above a fiducial energy density  $\rho_f$  [10]. The maximum mass inferred from this prescription is proportional to  $\rho_f^{-1/2}$ , but the compactness

limit is independent of  $\rho_f$  for  $\rho_f \ll \rho_c$ , where  $\rho_c$  is the central density of the star [9].

The central mass density of a star must be greater than the average density  $\rho_* = 3M/(4\pi R^3)$ , the value for a uniform density star with the same mass and radius. A firm lower limit to the density can be established if an upper limit to  $R$  exists. One observational limitation originates from the most rapidly spinning pulsar, PSR B1937 + 21 [11], which has a frequency  $\nu = 641 \text{ Hz}$ . This leads to a lower limit to  $M/R^3$  [12] and a lower limit

$$\rho_{c,\text{rot}} \approx 1.79 \times 10^{14} (\nu/641 \text{ Hz})^2 \text{ g cm}^{-3}, \quad (2)$$

which is, however, not very restrictive. A far more stringent limit could be achieved from a redshift observed from a neutron star. The largest observed redshift  $z_{\text{obs}}$  sets a lower limit to  $M/R$ , implying

$$\rho_{c,z} > \frac{3}{4\pi M^2} \left( \frac{c^2 z_{\text{obs}} (2 + z_{\text{obs}})}{2G(1 + z_{\text{obs}})^2} \right)^3. \quad (3)$$

Recently,  $z_{\text{obs}} = 0.35$  was reported [13] for the x-ray bursting source XTE J1814 – 338. With this value,

$$\rho_{c,z} > 1.69 \times 10^{15} (M_{\odot}/M)^2 \text{ g cm}^{-3}. \quad (4)$$

The central question is, how much greater can  $\rho_c$  be compared to any of the above expressions for physically motivated EOS? The answer to this question sets an upper limit to the density inside a star of a given mass. An important consequence of the existence of an upper limit is that the largest measured neutron star mass would set an upper limit to the density of cold matter. (In a dynamical environment, such as the gravitational collapse of a stellar core to a black hole or a high energy heavy ion collision, matter becomes hot and may achieve higher densities.) Additionally, one could infer whether or not non-nucleonic degrees of freedom, such as hyperons, Bose condensates, or quarks, which generally reduce the maximum mass, can exist in the cores of neutron stars.

Some insight can be gained by comparing analytical solutions to Einstein's equations with numerical solutions employing model EOS. The known analytic solutions fall into two classes: (i) the class that describes "normal" neutron stars for which  $\rho_c$  vanishes at the surface where

the pressure vanishes and (ii) the class that describes “self-bound” stars for which  $\rho_c$  is finite at the surface. In the first class, there are only three known analytic solutions: the Tolman VII solution [5], the Buchdahl solution [14], and the Nariai IV solution [15]. In the second class, an infinite number of analytic solutions exist, but the useful ones are variants of the Tolman IV and VII solutions [5,16], as well as the uniform density case [17].

All known analytic solutions are scale-free; they depend parametrically on the compactness ratio  $\beta = GM/Rc^2$ . However, by coupling these solutions with Eq. (1), i.e., by setting the compactness  $\beta = \beta_c \equiv 1/2.94$ , one can obtain relations between  $\rho_c$  and  $M$ . Dimensional arguments imply that  $\rho_c \propto M/(GM/c^2)^3 \propto M^{-2}$ . These relations for known analytic cases are as follows:

1. *Tolman VII*—This solution stems from the ansatz [5]

$$\rho = \rho_c[1 - (1 - w)(r/R)^2], \quad (5)$$

where the parameter  $w = \rho_s/\rho_c$  is the ratio of the energy densities at the surface and the center, which can vary between 0 and 1. (The case  $w = 1$  represents the uniform density fluid.) This leads to

$$\begin{aligned} \rho_{c,\text{VII}} &= \frac{15}{4\pi(2+3w)} \left(\frac{c^2\beta_c}{G}\right)^3 \frac{1}{M^2} \\ &\simeq \frac{1.45 \times 10^{16}}{(1+1.5w)} \left(\frac{M_\odot}{M}\right)^2 \text{ g cm}^{-3}. \end{aligned} \quad (6)$$

This solution is valid, in the case  $w = 0$  (the normal neutron star case), for  $\beta < 0.3862 \simeq 1/2.59$ . For positive  $w$  (the self-bound case), the solution is valid for larger values of  $\beta$ . Thus, this solution is useful for the case  $\beta = \beta_c$ . For  $w > 0$ , the central density decreases for a given mass relative to the normal neutron star case.

2. *Buchdahl*—This solution uses the EOS ansatz  $\rho c^2 = 12\sqrt{p_*P} - 5P$ , where  $p_*$  is a constant. In this case [14]

$$\begin{aligned} \rho_{c,\text{Buch}} &= \frac{\pi(2-5\beta_c)(1-\beta_c)^2}{8(1-2\beta_c)} \left(\frac{c^2\beta_c}{G}\right)^3 \frac{1}{M^2} \\ &\simeq 3.89 \times 10^{15} (M_\odot/M)^2 \text{ g cm}^{-3}. \end{aligned} \quad (7)$$

However, because Buchdahl’s solution is invalid when  $\beta \geq 1/5$ , the value for which the central sound speed becomes infinite, it cannot be used for the case  $\beta = \beta_c$ .

3. *Nariai IV*—This solution is characterized by [15]

$$\begin{aligned} \rho_{c,\text{NIV}} &= \frac{3}{8\pi} \left[ (\alpha - 1) \cos\sqrt{3\beta_c} + \frac{(6-\alpha)}{\sqrt{3\beta_c}} \sin\sqrt{3\beta_c} \right] \\ &\quad \times \left(\frac{c^2\beta_c}{G}\right)^3 \frac{1}{M^2} \\ &\simeq 9.88 \times 10^{15} (M_\odot/M)^2 \text{ g cm}^{-3}. \end{aligned} \quad (8)$$

Here,

$$\alpha = \frac{12 + \beta_c}{2 + \beta_c + 2\sqrt{1 - 2\beta_c}}. \quad (9)$$

This solution is valid for  $\beta < 0.4126$ , the value for which the central pressure and sound speed become infinite. This solution can also be generalized to include self-bound stars, and as for the Tolman VII case, the central density for a given mass decreases from that of Eq. (12) as the ratio  $w$  is increased from 0.

4. *Tolman IV (generalized)*—Lake [16] showed that the ansatz for the metric function

$$e^{\nu(r)} = \frac{[N - \beta(2N + 1) + \beta(r/R)^2]^N}{N^N(1 - 2\beta)^{N-1}}, \quad (10)$$

where  $N$  is a positive integer, produces an infinite family of analytic solutions of the self-bound type. Four of

these were previously known ( $N = 1, 3, 4$ , and  $5$ ). The case  $N = 1$  cannot properly be applied to our problem as this solution is finite only for  $\beta < 1/3$ . The most relevant case is for  $N = 2$ , for which  $c_s \approx \sqrt{1/3}$  throughout most of the star, similar to the behavior of strange quark matter. For this case,

$$\begin{aligned} \rho_{c,\text{TIV}} &= \frac{3}{4\pi} \left(\frac{2 - 2\beta_c}{2 - 5\beta_c}\right)^{2/3} \left(\frac{c^2\beta_c}{G}\right)^3 \frac{1}{M^2} \\ &\simeq 1.56 \times 10^{16} (M_\odot/M)^2 \text{ g cm}^{-3}. \end{aligned} \quad (11)$$

This solution is valid for  $\beta < 2/5$ . The ratio of the surface to the central densities for the case  $N = 2$  is

$$w = \frac{6 - 10\beta}{3} \left(\frac{2 - 5\beta}{2 - 2\beta}\right)^{2/3}, \quad (12)$$

which is approximately 0.32 for  $\beta = \beta_c$ . With increasing  $N$ , the central density for a given mass decreases from that of Eq. (11), and in the limit  $N \gg 1$ ,  $\rho_{c,\text{TIV}}(M)$  approaches the uniform density result.

To investigate the relevance of analytic relations between the central density and mass, we carried out numerical integrations of the Tolman-Oppenheimer-Volkoff structure equations for a multitude of EOS, including potential and field-theoretical models, and models that contain strong softening due to the occurrence of hyperons, Bose condensates, or quark matter, including the case of self-bound strange quark matter stars. The EOS were chosen from Refs. [18]. Figure 1 displays the maximum masses and the central energy densities of the maximum mass configurations. Analytic solutions for the upper limits from the Tolman VII normal neutron star case ( $w = 0$ ), the Tolman IV case for  $N = 2$ , and the redshift lower limit from Eq. (4) are also displayed. The paths of other analytic solutions are not shown for clarity, but they scale from the cases shown in Fig. 1.

It is fortuitous but significant that the Tolman VII solution forms a strict upper limit to the density of a maximum mass star, for each of the EOS displayed. We therefore

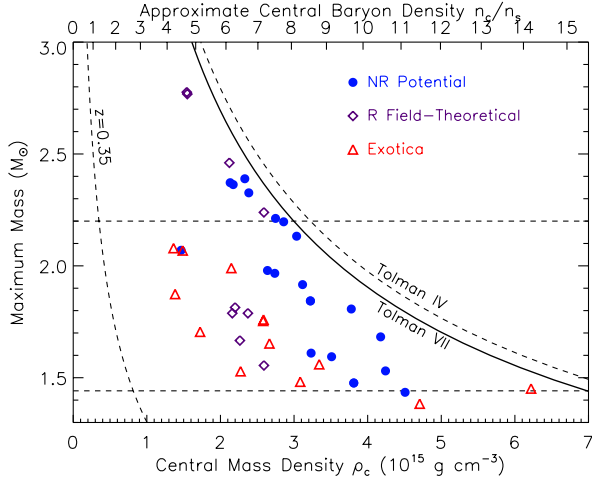


FIG. 1 (color online). The central energy density and mass of maximum mass configurations. Symbols reflect the nature of the EOS selected from Ref. [18]. NR are nonrelativistic potential models, R are field-theoretical models, and exotica refers to NR or R models in which strong softening occurs, due to the occurrence of hyperons, a Bose condensate, or quark matter. The exotica points include self-bound strange quark matter stars. For comparison, the central density–maximum mass relations for the redshift, Tolman VII ( $w = 0$ ), and Tolman IV ( $N = 2$ ) bounds from Eqs. (4), (6), and (11) are shown. The dashed lines for  $1.44M_\odot$  and  $2.2M_\odot$  serve to guide the eye.

conjecture that the Tolman VII curve marks the upper limit to the energy density inside a star of the indicated mass. Since the maximum density achievable with a given EOS is the central density of the maximum mass star, a stellar mass measurement can be directly converted into an upper limit for the maximum density. Since the measured mass must necessarily be less than the neutron star maximum mass, this limit also forms an absolute upper density inside any compact star. In other words, except in transient situations such as the big bang or in relativistic heavy ion collisions, this curve displays the ultimate density of cold baryonic matter.

All observed neutron stars with known masses have structurally insignificant rotation and magnetic fields. Nevertheless, we verified, using axially symmetric general relativistic structural computations from Ref. [19], that stars with rotation rates up to the Keplerian (mass-shedding) rate and magnetic fields up to the hydrostatic stability limit also satisfied the Tolman VII limit.

The above results are given in terms of the central mass or energy density  $\rho$ . However, most models of dense matter are formulated in terms of the baryon number density  $n$ . A good rule of thumb for converting  $\rho$  to  $n$ , using  $n_s \approx 0.16 \text{ fm}^{-3}$ , is

$$\rho/\rho_s \approx 0.9(n/n_s)[1 + 0.11(n/n_s)^{3/4}]. \quad (13)$$

The number density so obtained is indicated on the top

scale of Fig. 1. We emphasize that the plotted points are positioned using  $\rho_c$ , not  $n_c$ , in this figure.

The most accurately measured neutron star masses are from timing observations of radio binary pulsars [2,3]. These include pulsars orbiting another neutron star, a white dwarf, or a main-sequence star. Measured masses with  $1\sigma$  uncertainties are summarized in Fig. 2. Ordinarily, observations of pulsars in binaries yield orbital sizes and periods from Doppler phenomenon, from which the total mass of the binary can be deduced. But the compact nature of several binary pulsars permits detection of relativistic effects, such as Shapiro delay or orbit shrinkage due to gravitational radiation reaction, which constrains the inclination angle and permits measurement of each mass in the binary. The largest accurately measured mass originates from the binary pulsar system PSR 1913 + 16, whose masses are  $1.3867 \pm 0.0002M_\odot$  and  $1.4414 \pm 0.0002M_\odot$ , respectively [34].

Mass determinations in binaries with white dwarf companions show a broader mass range than binary pulsars having neutron star companions. Reference [37] suggests

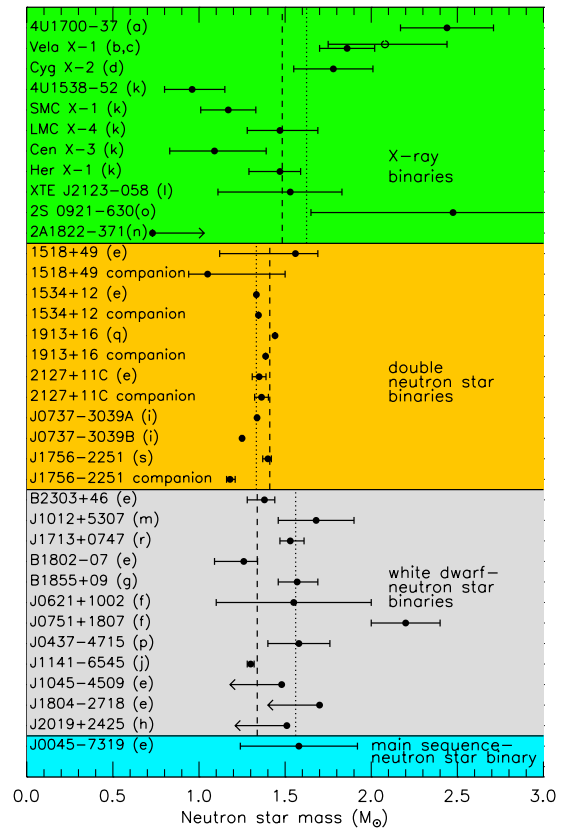


FIG. 2 (color online). Measured and estimated masses of neutron stars in radio binary pulsars and in x-ray accreting binaries. Sources are listed by letter (Refs. [20–36]). Error bars are  $1\sigma$ . Vertical dotted lines show average masses of each group ( $1.62M_\odot$ ,  $1.33M_\odot$ , and  $1.56M_\odot$ ); dashed vertical lines indicate inverse error weighted average masses ( $1.48M_\odot$ ,  $1.41M_\odot$ , and  $1.34M_\odot$ ).

that a narrow set of evolutionary circumstances conspires to form double neutron star binaries, leading to a restricted range of neutron star masses. The implication of this restriction for other binaries remains to be explored. The simple mean of the measured neutron star masses in white dwarf-neutron star binaries exceeds that of the double neutron star binaries by about  $0.23M_{\odot}$  (Fig. 2). A few cases of white dwarf binaries that contain neutron stars considerably larger than  $1.4M_{\odot}$  have been reported, although the  $2\sigma$  errors of most of these systems extend below  $1.4M_{\odot}$ . A striking case is PSR J0751 + 1807 [4] in which the estimated mass with  $1\sigma$  error bars is  $2.2 \pm 0.2M_{\odot}$ , and a mass of  $1.4M_{\odot}$  is  $4\sigma$  away. If this mass determination holds up after further observations, the central density constraints become intriguingly close to the estimated density for the quark-hadron phase transition. Raising the limit for the neutron star maximum mass could also mark the boundaries of other families of EOS in which substantial softening begins around  $2n_s$  to  $3n_s$ . This is significant, since exotica generally reduce the maximum mass appreciably.

Masses can also be estimated for binaries which contain an accreting neutron star emitting x rays. Some of these stars are characterized by relatively large masses but also large estimated errors (Fig. 2). The system Vela X-1 is noteworthy, because its lower mass limit ( $1.6M_{\odot}$  to  $1.7M_{\odot}$ ) is constrained, albeit mildly, by geometry [22]. The source 4U 1700 – 37 might be a black hole, due to lack of oscillations in its x-ray spectrum [20]. Another high-mass object, 2S 0921 – 630 [32], could be either a neutron star or a low-mass black hole. These latter two objects could play a significant role in determining the neutron star maximum and the black hole minimum masses.

This work was supported in part by U.S. DOE Grant No. DE-FG02-87ER-40317.

- 
- [1] S. E. Thorsett and D. Chakrabarty, *Astrophys. J.* **512**, 288 (1999) (e).
- [2] I. H. Stairs, *Science* **304**, 547 (2004).
- [3] R. N. Manchester, *Science* **304**, 542 (2004).
- [4] D. J. Nice, E. M. Splaver, and I. H. Stairs, astro-ph/0311296; (private communication) (f).
- [5] R. C. Tolman, *Phys. Rev.* **55**, 364 (1939).
- [6] J. R. Oppenheimer and G. B. Volkoff, *Phys. Rev.* **55**, 374 (1939).
- [7] H. A. Buchdahl, *Phys. Rev.* **116**, 1027 (1959); *Astrophys. J.* **146**, 275 (1966); H. Bondi, *Proc. R. Soc. London A* **282**, 303 (1964).
- [8] N. K. Glendenning, *Phys. Rev. D* **46**, 1274 (1992).
- [9] J. M. Lattimer, M. Prakash, D. Masak, and A. Yahil, *Astrophys. J.* **355**, 241 (1990).
- [10] C. E. Rhoades and R. Ruffini, *Phys. Rev. Lett.* **32**, 324 (1974).
- [11] M. Ashworth, A. G. Lyne, and F. G. Smith, *Nature (London)* **301**, 313 (1983).
- [12] J. M. Lattimer and M. Prakash, *Science* **304**, 536 (2004).
- [13] J. Cottam, F. Paerels, and M. Mendez, *Nature (London)* **420**, 51 (2002).
- [14] H. A. Buchdahl, *Astrophys. J.* **147**, 310 (1967).
- [15] H. Nariai, *Sci. Rep. Tohoku Univ. Ser. I* **34**, 160 (1950); **35**, 62 (1951).
- [16] K. Lake, *Phys. Rev. D* **67**, 104015 (2003).
- [17] K. Schwarzschild, *Sitzungsber. Dtsch. Akad. Wiss. Berlin, Kl. Math. Phys. Tech.* 189 (1916).
- [18] J. M. Lattimer and M. Prakash, *Astrophys. J.* **550**, 426 (2001); A. W. Steiner, M. Prakash, and J. M. Lattimer, *Phys. Lett. B* **486**, 239 (2000); M. Alford and S. Reddy, *Phys. Rev. D* **67**, 074024 (2003).
- [19] C. Cardall, M. Prakash, and J. M. Lattimer, *Astrophys. J.* **554**, 322 (2001).
- [20] J. S. Clark *et al.*, *Astron. Astrophys.* **392**, 909 (2002) (a).
- [21] O. Barziv *et al.*, *Astron. Astrophys.* **377**, 925 (2001) (b).
- [22] H. Quaintrell *et al.*, *Astron. Astrophys.* **401**, 313 (2003) (c).
- [23] J. A. Orosz and E. Kuulkers, *Mon. Not. R. Astron. Soc.* **305**, 132 (1999) (d).
- [24] D. J. Nice, E. M. Splaver, and I. H. Stairs, in *Radio Pulsars*, edited by M. Bailes, D. J. Nice, and S. E. Thorsett, *Astron. Soc. Pac. Conf. No. 302* (Astronomical Society of the Pacific, San Francisco, 2003), p. 75 (g).
- [25] D. J. Nice, E. M. Splaver, and I. H. Stairs, *Astrophys. J.* **549**, 516 (2001) (h).
- [26] A. G. Lyne *et al.*, *Science* **303**, 1153 (2004) (i).
- [27] M. Bailes *et al.*, *Astrophys. J.* **595**, L49 (2003) (j).
- [28] M. H. van Kerkwijk, J. van Paradijs, and E. J. Zuiderwijk, *Astron. Astrophys.* **303**, 497 (1995) (k).
- [29] D. M. Gelino, J. A. Tomsick, and W. A. Heindl, *Bull. Am. Astron. Soc.* **34**, 1199 (2003); J. A. Tomsick (private communication) (l).
- [30] Ch. Lange *et al.*, *Mon. Not. R. Astron. Soc.* **326**, 274 (2001) (m).
- [31] P. G. Jonker, M. van der Klis, and P. J. Groot, *Mon. Not. R. Astron. Soc.* **339**, 663 (2003) (n).
- [32] P. G. Jonker, D. Steeghs, G. Nelemans, and M. van der Klis, *Mon. Not. R. Astron. Soc.* **356**, 621 (2005) (o).
- [33] W. van Straten *et al.*, *Nature (London)* **412**, 158 (2001) (p).
- [34] J. M. Weisberg and J. H. Taylor, astro-ph/0407149 (q).
- [35] E. M. Splaver *et al.*, *Astrophys. J.* (to be published); astro-ph/0410488 (r).
- [36] A. J. Faulkner *et al.*, *Astrophys. J. Lett.* (to be published); astro-ph/0411796 (s).
- [37] H. A. Bethe and G. E. Brown, *Astrophys. J.* **506**, 780 (1998).